

Abstract

Observations of peroxyntic acid (HO_2NO_2) and nitric acid (HNO_3) were made during a 4 month period of Antarctic winter darkness at the coastal Antarctic research station, Halley. Mixing ratios of HNO_3 ranged from instrumental detection limits to ~ 8 parts per trillion by volume (pptv), and of HO_2NO_2 from detection limits to ~ 5 pptv; the average ratio of $\text{HNO}_3 : \text{HO}_2\text{NO}_2$ was $2.0(\pm 0.6) : 1$, with HNO_3 always present at greater mixing ratios than HO_2NO_2 during the winter darkness. An extremely strong association existed for the entire measurement period between mixing ratios of the respective trace gases and temperature: for HO_2NO_2 , $R^2 = 0.72$, and for HNO_3 , $R^2 = 0.70$. We focus on three cases with considerable variation in temperature, where wind speeds were low and constant, such that, with the lack of photochemistry, changes in mixing ratio were likely to be driven by adsorption/desorption mechanisms alone. We derived enthalpies of adsorption (ΔH_{ads}) for these three cases. The average ΔH_{ads} for HNO_3 was $-42 \pm 7 \text{ kJ mol}^{-1}$ and for HO_2NO_2 was $-56 \pm 3 \text{ kJ mol}^{-1}$; these values are extremely close to laboratory-derived values. This exercise demonstrates (i) that adsorption to/desorption from the snow pack should be taken into account when addressing budgets of boundary layer HO_2NO_2 and HNO_3 at any snow-covered site, and (ii) that Antarctic winter can be used as a natural “laboratory in the field” for testing data on physical exchange mechanisms.

1 Introduction

Peroxy nitric acid (HO_2NO_2 , also written as HNO_4) and nitric acid (HNO_3) are acidic gases that are of increasing interest to polar tropospheric chemistry. Their primary relevance is that they act as reservoir species for HO_x and NO_x , which are now recognised to drive the surprisingly vigorous oxidation chemistry that has been observed during Antarctic summer (e.g. Davis et al., 2001; Chen et al., 2001). The spatial and temporal distribution of HO_2NO_2 and HNO_3 across the polar regions thus becomes important

ACPD

14, 12771–12796, 2014

HO_2NO_2 and HNO_3 in the coastal Antarctic winter night

A. E. Jones et al.

Title Page

Abstract

Introduction

Conclusions

References

Tables

Figures



Back

Close

Full Screen / Esc

Printer-friendly Version

Interactive Discussion



for understanding the overall atmospheric chemical system, and models require details of their sources, and any physical exchange process by which they move from one environmental compartment to another. Currently, many of these details are unknown.

The gas-phase chemistry of HO₂NO₂ and HNO₃ is relatively straightforward. Peroxy nitric acid is a somewhat unstable molecule that forms and dissociates through its temperature-dependent equilibrium reaction:



which renders an increased stability for HO₂NO₂ at lower temperatures.

There are a number of photodissociation pathways, of which the most important are thought to be:



Peroxynitric acid can also be lost through reaction with OH:



Gas-phase production of nitric acid proceeds via:



The major loss processes are reaction with OH and photolysis:



Both HO₂NO₂ (Ulrich et al., 2012) and HNO₃ (Bartels-Rausch et al., 2002; Hudson et al., 2002; Ullerstam et al., 2005) have been shown in laboratory experiments to adsorb to ice surfaces. This conclusion is supported by field observations which have confirmed uptake of both HNO₃ and HO₂NO₂ to snow surfaces (Huey et al., 2004; Slusher et al., 2002), and of HNO₃ to cirrus clouds (Weinheimer et al., 1998; Popp et al., 2004;

Ziereis et al., 2004). In general, therefore, in snow covered areas, or indeed regions of the atmosphere with lofted snow/ice, such as cirrus clouds or blowing/precipitating snow, physical adsorption of HNO_3 and HO_2NO_2 from the air to the snow/ice is likely to occur. The details of this uptake will differ somewhat between the two molecules, as the enthalpy of adsorption for HO_2NO_2 is greater than for HNO_3 (Ulrich et al., 2012), and both adsorption processes are temperature-dependent (Crowley et al., 2010; Ulrich et al., 2012).

High resolution observations of HNO_3 and HO_2NO_2 in the polar regions are scarce. Critically, both HO_2NO_2 and HNO_3 have been measured together during a number of Antarctic studies at high temporal resolution. These studies have included both ground-based experiments at South Pole (Slusher et al., 2002; Huey et al., 2004) and airborne measurements across the wider Antarctic Plateau (Slusher et al., 2010).

The ground-based studies have revealed considerable inter-annual variability in summertime HNO_3 and HO_2NO_2 mixing ratios, but always of the order 10s pptv at the South Pole. For example, the median observed HNO_3 between 16 and 31 December in 2000 was 18.2 pptv and for HO_2NO_2 was 23.5 pptv (Davis et al., 2004); over the equivalent time period in 2003, the median HNO_3 was 84 pptv, and for HO_2NO_2 was 39 pptv (Eisele et al., 2008). Considerably greater mixing ratios have also been observed; for example, the median mixing ratio of HNO_3 between 15 and 30th November 2003 was 194 pptv, and of HO_2NO_2 was 63 pptv (Eisele et al., 2008). These high mixing ratios are fuelled by in situ production from elevated levels of NO_x and HO_x within the South Pole boundary layer, in turn driven by photochemical release of trace gases from the surrounding snowpack (Davis et al., 2001, 2008).

The airborne measurements assessed the three-dimensional distribution of HO_2NO_2 and HNO_3 across the Antarctic Plateau during the ANTCI 2005 campaign (Slusher et al., 2010). They revealed significant vertical gradients in both species, with higher concentrations at the ground, consistent with a source associated with emissions from the snowpack. The measurements also showed a widespread distribution of both HNO_3 and HO_2NO_2 across the Plateau region.

HO_2NO_2 and HNO_3 in the coastal Antarctic winter night

A. E. Jones et al.

[Title Page](#)[Abstract](#)[Introduction](#)[Conclusions](#)[References](#)[Tables](#)[Figures](#)[Back](#)[Close](#)[Full Screen / Esc](#)[Printer-friendly Version](#)[Interactive Discussion](#)

HO₂NO₂ and HNO₃ in the coastal Antarctic winter night

A. E. Jones et al.

Title Page

Abstract

Introduction

Conclusions

References

Tables

Figures



Back

Close

Full Screen / Esc

Printer-friendly Version

Interactive Discussion



To date there have been no measurements of high temporal resolution HO₂NO₂ and HNO₃ in coastal Antarctica, and no measurements at all from Antarctica outside the summer season. We report here observations of HO₂NO₂ and HNO₃ made using a chemical ionisation mass spectrometer (CIMS) at Halley research station in coastal Antarctica (75°35' S, 26°39' W) from 24 May to 18 September 2007. The data allow us to assess whether HNO₃ and HO₂NO₂ are present in significant concentrations at other Antarctic locations and seasons than the Antarctic Plateau in summer. They also provide an opportunity to test laboratory-derived physical exchange parameters under semi-constrained, but genuine real-world conditions. At Halley, the sun remains below the horizon from 30 April to 13 August, such that this new data set includes many weeks of winter darkness. Under these conditions of 24 h per day darkness, atmospheric photochemistry stalls, and trace gas concentrations are controlled entirely by either transport or physical air-snow exchange.

2 Experimental

2.1 CIMS data

The CIMS instrument used in this study has been described in detail elsewhere (Buys et al., 2013). It was installed in the Clean Air Sector Laboratory (CASLab), which is located roughly 1 km from the main Halley station, and in a sector that rarely receives air from the base (Jones et al., 2008). The CIMS inlet extended ~ 20 cm above the roof of CASLab, at a height roughly 5 m above the surrounding snowpack. The inlet system was designed to minimise residence time and surface losses (Neuman et al., 1999).

The instrument employed the SF₆⁻ method to detect both HNO₃ and HO₂NO₂, using the NO₄⁻(HF) cluster at *m/z* 98 to detect HO₂NO₂, and NO₃⁻(HF) at *m/z* 82 to detect HNO₃. Background measurements, or zeros, were obtained every 10 min. These were achieved by passing sampled air for 3 min through a customized filter filled with activated coarse charcoal and nylon glass wool coated in NaHCO₃. This scrubbing method

has previously been shown to be efficient at removing both HO₂NO₂ and HNO₃ from sampled air (Slusher et al., 2001). The instrument detection limit derived from background data averaged over 10 min was 0.7 pptv for HNO₃ and 0.4 pptv for HO₂NO₂.

While the SF₆⁻ method has been used successfully in previous field campaigns (e.g. Slusher et al., 2002, 2010), it has been demonstrated in laboratory studies (Slusher et al., 2001) that SF₆⁻ reacts with H₂O in the sample air flow. This introduces an interferent into the technique, the non-linearity of which is evident in the unfiltered data (not shown). However, Slusher et al. (2001) also concluded that this interferent was significant only at dewpoints greater than -25 °C, and that at lower dewpoints, the interferent was negligible. During the period of measurements at Halley, dewpoint temperatures varied from -12 °C to -52 °C (mean -31 °C), but were below -25 °C for 81 % of the time. To remove the potential for H₂O interference in our data, all measurements made at dewpoints above -25 °C are filtered out from the dataset.

2.2 Boundary layer meteorology

Measurements of near-surface boundary layer meteorology were made on a 32 m profiling mast located ~ 25 m from the CASLab. Bulk sensors were located at 1, 2, 4, 8, 16, and 32 m a.g.l., recording at 1 Hz and averaged to 10 min means; temperatures and humidity were measured with platinum resistance thermometers (0.1 K resolution) and solid state humidity probes (2 % resolution), respectively, using an aspirated HMP35D from Vaisala Corp. Ten min vector average wind speed and direction were measured with R.M Young propeller vanes at 0.1 m s⁻¹ and 2° resolution.

Three 3-axis Metek USA-1 ultrasonic anemometer/thermometers were deployed at the 4, 16, and 32 m levels, sampling at 20 Hz. The data were tilt corrected and the relevant co-variances calculated over 1 min means.

Title Page

Abstract

Introduction

Conclusions

References

Tables

Figures



Back

Close

Full Screen / Esc

Printer-friendly Version

Interactive Discussion



correlation coefficients with temperature are high, with $R^2 = 0.70$ and 0.72 for HNO_3 and HO_2NO_2 respectively.

Given that mixing ratios of HNO_3 and HO_2NO_2 are so strongly associated with ambient temperature, Table 1 gives the mean and standard deviation of HNO_3 and HO_2NO_2 measured between 24 May and 18 September 2007, calculated within specific temperature ranges. The statistics are derived using only the filtered data that were above 3-sigma detection limits. At South Pole during the summer, ambient temperature ranged from -31.5°C to -23.6°C , with a mean of -27.7°C ; within this temperature range, HNO_3 mixing ratios ranged from < 5 to 54 pptv (mean 25 pptv) and HO_2NO_2 ranged from < 5 to 68 pptv (mean 22 pptv). For the equivalent temperature range at Halley (also with a mean of -27.7°C), mean and maximum mixing ratios for HNO_3 were 4.4 pptv and 9 pptv respectively, and for HO_2NO_2 were 2.5 pptv and 5 pptv respectively, clearly significantly below those observed at South Pole, for the reasons outlined above.

Differences between South Pole summer and Halley winter are also evident in the ratio of $\text{HNO}_3 : \text{HO}_2\text{NO}_2$. Throughout the Halley measurement period, the average ratio of $\text{HNO}_3 : \text{HO}_2\text{NO}_2$ was $2.0(\pm 0.6) : 1$, with HNO_3 always (apart from a few outliers) present at greater mixing ratios than HO_2NO_2 during the winter darkness (see Fig. 4). This finding is in contrast to observations from South Pole during sunlit summer time, when mixing ratios of HNO_3 and HO_2NO_2 were roughly equal for much of the measurement period (Slusher et al., 2002). Figure 1 of Slusher et al. (2002) shows that HO_2NO_2 was present at higher mixing ratios than HNO_3 for roughly 2 out of the 7 days of measurements; during the roughly 4 months of measurements at Halley, the only occasion when the mixing ratio of HO_2NO_2 exceeded that of HNO_3 was on the 6 and 7 September, a period when temperatures were particularly low but there was a limited amount of sunlight.

HO_2NO_2 and HNO_3 in the coastal Antarctic winter night

A. E. Jones et al.

Title Page

Abstract

Introduction

Conclusions

References

Tables

Figures



Back

Close

Full Screen / Esc

Printer-friendly Version

Interactive Discussion



3.2 Short-term variability in HNO₃ and HO₂NO₂ and link to ambient temperature

The short-term variability in the HNO₃ and HO₂NO₂ is shown more clearly in Fig. 5. The three examples show periods when ambient air temperatures varied rapidly and considerably, but where they remained below the -25°C dewpoint threshold such that no chemical data filtering was required. These 10 min averages show that even very small-scale features of temperature change are reflected in the chemical measurements. For example, at midnight on 5 June, the short-lived peak in temperature is reflected also in HNO₃ and HO₂NO₂; the temperature peak around 11 a.m. on 21 June is apparent with similar, small, peaks in HNO₃ and HO₂NO₂; and the short-lived temperature peak around noon on 15 July is also evident in short-lived increases in HNO₃ and HO₂NO₂ mixing ratios. While large-scale variability in HNO₃ and HO₂NO₂ could be linked to air mass origin, such fine-scale variability can only be explained by a local, fast-acting, source/sink mechanism. The association between variability in HNO₃ and HO₂NO₂ and changes in ambient temperature strongly suggest a temperature-dependent mechanism. Given our understanding of the interaction between acidic gases and ice gained through laboratory studies (e.g. Huthwelker et al., 2006), the most likely mechanism is temperature-dependent adsorption/desorption at the snow surface.

3.3 Evidence for HO₂NO₂ and HNO₃ air/snow exchange

To probe in more detail the response of HNO₃ and HO₂NO₂ to changes in temperature, we examined periods in the data where ambient temperatures changed, but where wind speeds were relatively low and invariable. By adopting this approach, we minimise any influence that air flow through the snow (e.g. via ventilation/wind pumping) may have on air/snow exchange processes. We derive a mixing diffusivity to determine the timescale for vertical mixing (via turbulent diffusion) between the snow surface and the CIMS inlet height, in order to confirm that the CIMS HNO₃ and HO₂NO₂ observations can be used to analyse processes occurring at the ground-level air/snow interface. The mixing diffusivity is roughly equal to $k \cdot z \cdot u_*$, where k = von Karman's constant (= 0.4),

Title Page

Abstract

Introduction

Conclusions

References

Tables

Figures



Back

Close

Full Screen / Esc

Printer-friendly Version

Interactive Discussion



HO₂NO₂ and HNO₃ in the coastal Antarctic winter night

A. E. Jones et al.

Title Page

Abstract

Introduction

Conclusions

References

Tables

Figures



Back

Close

Full Screen / Esc

Printer-friendly Version

Interactive Discussion



z = CIMS inlet height (= 5 m) and u_* , the friction velocity, is derived from the sonic anemometer data (Stull, 1988). The e-folding time scale, t_{sc} , is given by $z^2/\text{diffusivity}$, that is $t_{sc} = z/(k \cdot u_*)$. t_{sc} will vary during each case study, but cannot be negative: this range is presented below derived from log means and standard deviations. Figure 6a shows observations made on 30 May 2007, with a clear gradual increase in both HNO₃ and HO₂NO₂ as ambient temperatures rose from $\sim -44^\circ\text{C}$ to $\sim -30^\circ\text{C}$. On this day, data from the boundary layer mast (not shown) show that between the surface and 8 m height, there was little or no temperature gradient; to first order, therefore, 8 m temperatures can be used as a surrogate for those at the ground. Wind speeds were between 0 and 2 m s^{-1} from the surface to 4 m, and remained at around 2 m s^{-1} at 8 m height. For 95 % of the time, t_{sc} was between 100 and 300 s.

Figure 6b shows data for the period from 9 a.m. to midnight on 21 June, discussed briefly in Sect. 3.2 above. Again, a gradual increase in mixing ratios of HNO₃ and HO₂NO₂ is evident (upper panel), as ambient temperatures rose gradually from $\sim -38^\circ\text{C}$ to $\sim -26^\circ\text{C}$. Data from the boundary layer met mast show that, during this period, there was no vertical gradient in temperature between the surface and 8 m height; wind speeds from the surface to 8 m were below 2 m s^{-1} . Data from the sonic anemometers show that vertical mixing was again very weak, with mixing time scales between 90 and 600 s.

Figure 6c shows observations from midnight to 9 a.m. on 18 July, another quiescent period, with wind speeds in the lowest 8 m below 1 m s^{-1} , and with no temperature gradient below 32 m. Gradual increases in both HNO₃ and HO₂NO₂ proceed as ambient temperatures rise from -38°C to -30°C . t_{sc} varied between 30 and 100 s during the event.

Correlation coefficients between mixing ratios of HNO₃ (and HO₂NO₂) and temperature, are extremely high for the time periods presented in Fig. 6: R^2 for the correlation between HNO₃ and temperature is 0.72 (30 May), 0.90 (21 June) and 0.72 (18 July); for the correlation between HO₂NO₂ and temperature, R^2 was 0.88 (30 May), 0.94 (21 June), and 0.92 (18 July). The values of R^2 show that between 72 % and 90 % of the

variability in HNO₃ can be explained by variability in temperature; and between 88 % and 94 % of the variability in HO₂NO₂ can be explained by the variability in temperature.

3.4 Deriving enthalpy of adsorption from the Halley field data

The enthalpies of adsorption between HNO₃/ice and HO₂NO₂/ice have been derived in laboratory experiments carried out under environmentally-relevant conditions. Ulrich et al. (2012) studied uptake of HO₂NO₂ at low concentrations and temperatures between 230 K and 253 K while Bartels-Rausch et al. (2002) studied the adsorption enthalpy of HNO₃. Field studies carried out during the 24 h per day darkness of Antarctic winter provide optimum conditions for validating such laboratory-derived physical air/snow exchange parameters under “real-world” conditions.

At equilibrium, the partitioning of HO₂NO₂ or HNO₃ molecules between the gas phase (*C_g*) and the snow/ice surface (*C_s*) can be expressed as:

$$K_{\text{part}} = \frac{C_s}{C_g}$$

As the partition constant will obey the van't Hoff equation, a new equation can be written:

$$\frac{d \ln K_{\text{part}}}{d \frac{1}{T}} = - \frac{\Delta H_{\text{ads}}}{R}$$

where *T* is the temperature (K), ΔH is the enthalpy of adsorption (J mol⁻¹), *R* is the gas constant (8.314 J K⁻¹ mol⁻¹).

Given our definition of *K_{part}* above, the equation can then be re-formulated as:

$$\frac{d \ln \frac{C_s}{C_g}}{d \frac{1}{T}} = - \frac{\Delta H_{\text{ads}}}{R}$$

Title Page

Abstract

Introduction

Conclusions

References

Tables

Figures



Back

Close

Full Screen / Esc

Printer-friendly Version

Interactive Discussion



HO₂NO₂ and HNO₃ in the coastal Antarctic winter night

A. E. Jones et al.

Title Page

Abstract

Introduction

Conclusions

References

Tables

Figures



Back

Close

Full Screen / Esc

Printer-friendly Version

Interactive Discussion



At 240 K, roughly the temperatures of our observations, Ulrich et al. (2012), in their Fig. 4, show $C_s/C_g \approx 20$ cm for HO₂NO₂ and 8000 cm for HNO₃. In the firn, the ratio of the surface area of snow to the volume of air is approximately 0.5 to 5 cm⁻¹ (based on a density of snow of 0.7 and a specific surface area of 100 to 1000 m² kg⁻¹, Domine et al., 2008). We can therefore calculate that the ratio of the number of molecules of HNO₃ adsorbed to the snow surface to that in the gas phase, is approximately 4000 to 40 000; for HO₂NO₂, this ratio is 10 to 100. As a result, for both HNO₃ and HO₂NO₂, exchange between the air and snow will thus have little effect on C_s , which can therefore be considered as a constant relative to C_g .

If we also assume that, over several hours, and under low and constant wind conditions, the concentration at our inlet tracks the concentration in the firn, then:

$$\frac{d \ln C_g}{d \frac{1}{T}} = \frac{\Delta H_{\text{ads}}}{R}$$

It is then possible to derive ΔH_{ads} from the slope of $\ln C_g$ vs. $1/T$ multiplied by R .

For the Halley data, Fig. 7 shows plots of both $\ln(\text{HNO}_3)$ vs. $1/T$ and $\ln(\text{HO}_2\text{NO}_2)$ vs. $1/T$ for the time periods discussed in Sect. 3.3 above. As a reminder, these periods are characterised by 24 h per day darkness, low wind speeds, and limited vertical mixing from turbulent diffusion, so are as close to laboratory conditions as could be found in our dataset. They were also chosen as they spanned a reasonably large temperature range, which would improve the constraint on the linear fit.

The values of ΔH_{ads} derived from these fits are given in Table 2. The average ΔH_{ads} for HNO₃ is -42 ± 7 kJ mol⁻¹ which can be compared with the laboratory-derived value (Bartels-Rausch et al., 2002) of -44 kJ mol⁻¹; for HO₂NO₂, the average ΔH_{ads} is -56 ± 3 kJ mol⁻¹ which can be compared with the laboratory-derived value (Ulrich et al., 2012) of -59 kJ mol⁻¹. In both cases, the agreement between laboratory and field-derived enthalpies of adsorption is remarkably good.

4 Summary and conclusions

We present the first high time resolution observations of HNO_3 and HO_2NO_2 in coastal Antarctica, and the first from Antarctica during the dark winter period. Mixing ratios of HNO_3 ranged from instrumental detection limits to ~ 8 parts per trillion by volume (pptv) and of HO_2NO_2 varied from detection limits to ~ 5 pptv. These values are on average lower than those observed at South Pole in summer, where mixing ratios of HNO_3 and HO_2NO_2 were generally in the 10s of pptv, and sometimes over 100 pptv.

The Antarctic, during winter, is an ideal natural laboratory for studying physical air/snow exchange processes. The environmental system is considerably simplified compared with other times of the year because of the lack of photochemical activity which must otherwise be taken into account when interpreting data.

The measurements of HNO_3 and HO_2NO_2 presented here are entirely consistent with laboratory experiments showing a temperature-dependence in the partitioning of both HNO_3 and HO_2NO_2 to ice. They also support the conclusion that HO_2NO_2 /ice interactions are stronger than those between HNO_3 and ice, as shown by the higher enthalpy of adsorption of HO_2NO_2 compared with HNO_3 (Ulrich et al., 2012).

On short-timescales, therefore, HNO_3 and HO_2NO_2 that is adsorbed to snow/ice can be re-released as temperatures rise. The snowpack can thus act as a source of HNO_3 and HO_2NO_2 to the overlying atmosphere at all times of the year. Similarly, HNO_3 and HO_2NO_2 adsorbed to cirrus clouds would be desorbed should temperatures rise. Such a reversible, temperature-dependent partitioning also provides a mechanism for re-distributing HNO_3 and HO_2NO_2 on a local or regional scale across Antarctica. Snow can be transported considerable distances by storm systems, and adsorbed HO_2NO_2 and HNO_3 can be desorbed as a function of changing temperature experienced along the transport pathway.

While clearly a controlling mechanism during polar night, the importance of air/snow partitioning relative to photochemistry will vary according to time of year and location. However, adsorption to/desorption from the snow pack should be taken into account

ACPD

14, 12771–12796, 2014

HO_2NO_2 and HNO_3 in the coastal Antarctic winter night

A. E. Jones et al.

Title Page

Abstract

Introduction

Conclusions

References

Tables

Figures



Back

Close

Full Screen / Esc

Printer-friendly Version

Interactive Discussion



when addressing budgets of boundary layer HO₂NO₂ and HNO₃ at any snow-covered site, as all are likely to experience varying ambient temperature which would drive such air/snow exchange.

Acknowledgements. The authors thank G. Huey and D. Tanner for providing the CIMS instrument used in this work, and for their help in setting it up at Halley. A. E. Jones thanks R. Mulvaney for useful discussions around this work. This study is part of the British Antarctic Survey Polar Science for Planet Earth Programme. It was funded by The Natural Environment Research Council (NERC).

References

Bartels, T., Eichler, B., Zimmermann, P., Gäggeler, H. W., and Ammann, M.: The adsorption of nitrogen oxides on crystalline ice, *Atmos. Chem. Phys.*, 2, 235–247, doi:10.5194/acp-2-235-2002, 2002.

Bauguitte, S. J.-B., Bloss, W. J., Evans, M. J., Salmon, R. A., Anderson, P. S., Jones, A. E., Lee, J. D., Saiz-Lopez, A., Roscoe, H. K., Wolff, E. W., and Plane, J. M. C.: Summertime NO_x measurements during the CHABLIS campaign: can source and sink estimates unravel observed diurnal cycles?, *Atmos. Chem. Phys.*, 12, 989–1002, doi:10.5194/acp-12-989-2012, 2012.

Buys, Z., Brough, N., Huey, G., Tanner, D., von Glasow, R., and Jones, A. E.: High temporal resolution Br₂, BrCl and BrO observations in coastal Antarctica, *Atmos. Chem. Phys.*, 13, 1329–1343, doi:10.5194/acp-13-1329-2013, 2013.

Chen, G., Davis, D., Crawford, J., Nowak, J. B., Eisele, F., Mauldin, R. L., Tanner, D., Buhr, M., Shetter, R., Lefer, B., Arimoto, R., Hogan, A., and Blake, D.: An investigation of South Pole HO_x chemistry: comparison of model results with ISCAT observations, *Geophys. Res. Lett.*, 28, 3633–3636, 2001.

Cotter, E. S. N., Jones, A. E., Wolff, E. W., and Bauguitte, S. J.-B.: What controls photochemical NO and NO₂ production from Antarctic snow? Laboratory investigation assessing the wavelength and temperature dependence, *J. Geophys. Res.*, 108, D04147, doi:10.1029/2002JD002602, 2003.

Crowley, J. N., Ammann, M., Cox, R. A., Hynes, R. G., Jenkin, M. E., Mellouki, A., Rossi, M. J., Troe, J., and Wallington, T. J.: Evaluated kinetic and photochemical data for atmospheric

Title Page

Abstract

Introduction

Conclusions

References

Tables

Figures



Back

Close

Full Screen / Esc

Printer-friendly Version

Interactive Discussion



HO₂NO₂ and HNO₃ in the coastal Antarctic winter night

A. E. Jones et al.

[Title Page](#)[Abstract](#)[Introduction](#)[Conclusions](#)[References](#)[Tables](#)[Figures](#)[Back](#)[Close](#)[Full Screen / Esc](#)[Printer-friendly Version](#)[Interactive Discussion](#)

chemistry: Volume V – heterogeneous reactions on solid substrates, *Atmos. Chem. Phys.*, 10, 9059–9223, doi:10.5194/acp-10-9059-2010, 2010.

Davis, D., Nowak, J. B., Chen, G., Buhr, M., Arimoto, R., Hogan, A., Eisele, F., Mauldin, L., Tanner, D., Shetter, R., Lefer, B., and McMurry, P.: Unexpected high levels of NO observed at South Pole, *Geophys. Res. Lett.*, 28, 3625–3628, 2001.

Davis, D., Chen, G., Buhr, M., Crawford, J., Lenschow, D., Lefer, B., Shetter, R., Eisele, F., Mauldin, L., and Hogan, A.: South Pole NO_x chemistry: an assessment of factors controlling variability and absolute levels, *Atmos. Environ.*, 38, 5375–5388, 2004.

Davis, D. D., Seelig, J., Huey, G., Crawford, J., Chen, G., Wang, Y., Buhr, M., Helmig, D., Neff, W., Blake, D., Arimoto, R., and Eisele, F.: A reassessment of Antarctic plateau reactive nitrogen based on ANTCI 2003 airborne and ground based measurements, *Atmos. Environ.*, 42, 2831–2848, doi:10.1016/j.atmosenv.2007.07.039, 2008.

Domine, F., Albert, M., Huthwelker, T., Jacobi, H.-W., Kokhanovsky, A. A., Lehning, M., Picard, G., and Simpson, W. R.: Snow physics as relevant to snow photochemistry, *Atmos. Chem. Phys.*, 8, 171–208, doi:10.5194/acp-8-171-2008, 2008.

Eisele, F., Davis, D. D., Helmig, D., Oltmans, S. J., Neff, W., Huey, G., Tanner, D., Chen, G., Crawford, J., Arimoto, R., Buhr, M., Mauldin, L., Hutterli, M., Dibb, J., Blake, D., Brooks, S. B., Johnson, B., Roberts, J. M., Wang, Y., Tan, D., and Flocke, F.: Antarctic tropospheric chemistry investigation (ANTCI) 2003 overview, *Atmos. Environ.*, 42, 2749–2761, doi:10.1016/j.atmosenv.2007.04.013, 2008.

Hudson, P. K., Shilling, J. E., Tolbert, M. A., and Toon, O. B.: Uptake of nitric acid on ice at tropospheric temperatures: implications for cirrus clouds, *J. Phys. Chem. A*, 106, 9874–9882, 2002.

Huey, L. G., Tanner, D. J., Slusher, D. L., Dibb, J. E., Arimoto, R., Chen, G., Davis, D., Buhr, M. P., Nowak, J. B., Mauldin, R. L., Eisele, F. L., and Kosciuch, E.: CIMS measurements of HNO₃ and SO₂ at the South Pole during ISCAT 2000, *Atmos. Environ.*, 38, 5411–5421, 2004.

Huthwelker, T., Ammann, M., and Peter, T.: The uptake of acidic gases on ice, *Chem. Rev.*, 106, 1375–1444, 2006.

Jones, A. E., Wolff, E. W., Salmon, R. A., Bauguitte, S. J.-B., Roscoe, H. K., Anderson, P. S., Ames, D., Clemittshaw, K. C., Fleming, Z. L., Bloss, W. J., Heard, D. E., Lee, J. D., Read, K. A., Hamer, P., Shallcross, D. E., Jackson, A. V., Walker, S. L., Lewis, A. C., Mills, G. P., Plane, J. M. C., Saiz-Lopez, A., Sturges, W. T., and Worton, D. R.: Chemistry of the Antarctic

HO₂NO₂ and HNO₃ in the coastal Antarctic winter night

A. E. Jones et al.

[Title Page](#)[Abstract](#)[Introduction](#)[Conclusions](#)[References](#)[Tables](#)[Figures](#)[Back](#)[Close](#)[Full Screen / Esc](#)[Printer-friendly Version](#)[Interactive Discussion](#)

Boundary Layer and the Interface with Snow: an overview of the CHABLIS campaign, *Atmos. Chem. Phys.*, 8, 3789–3803, doi:10.5194/acp-8-3789-2008, 2008.

Kim, S., Huey, L. G., Stickel, R. E., Tanner, D. J., Crawford, J. H., Olson, J. R., Chen, G., Brune, W. H., Ren, X., Leshner, R., Wooldridge, P. J., Bertram, T. H., Perring, A., Cohen, R. C.,
5 Lefer, B. L., Shetter, R. E., Avery, M., Diskin, G., and Sokolik, I.: Measurement of HO₂NO₂ in the free troposphere during the intercontinental chemical transport experiment – North America 2004, *J. Geophys. Res.-Atmos.*, 112, D12S01, doi:10.1029/2006JD007676, 2007.

Neuman, J. A., Huey, L. G., Ryerson, T. B., and Fahey, D. W.: Study of inlet materials for sampling atmospheric nitric acid, *Environ. Sci. Technol.*, 33, 1133–1136, doi:10.1021/es980767f,
10 1999.

Popp, P. J., Gao, R. S., Marcy, T. P., Fahey, D. W., Hudson, P. K., Thompson, T. L., Karcher, B., Ridley, B. A., Weinheimer, A. J., Knapp, D. J., Montzka, D. D., Baumgardner, D., Garrett, T. J., Weinstock, E. M., Smith, J. B., Sayres, D. S., Pittman, J. V., Dhaniyala, S., Bui, T. P., and Mahoney, M. J.: Nitric acid uptake on subtropical cirrus cloud particles, *J. Geophys. Res.*,
15 109, D06302, doi:10.1029/2003JD004255, 2004.

Slusher, D. L., Pitteri, S. J., Haman, B. J., Tanner, D. J., and Huey, L. G.: A chemical ionization technique for measurement of pernitric acid in the upper troposphere and the polar boundary layer, *Geophys. Res. Lett.*, 28, 3875–3878, doi:10.1029/2001GL013443, 2001.

Slusher, D. L., Huey, L. G., Tanner, D. J., Chen, G., Davis, D. D., Buhr, M., Nowak, J. B., Eisele, F. L., Kosciuch, E., Mauldin, R. L., Lefer, B. L., Shetter, R. E., and Dibb, J. E.: Measurements of pernitric acid at the South Pole during ISCAT 2000, *Geophys. Res. Lett.*, 29,
20 2011, doi:10.1029/2002GL015703, 2002.

Slusher, D. L., Neff, W. D., Kim, S., Huey, L. G., Wang, Y., Zeng, T., Tanner, D. J., Blake, D. R., Beyersdorf, A., Lefer, B. L., Crawford, J. H., Eisele, F. L., Mauldin, R. L., Kosciuch, E., Buhr, M. P., Wallace, H. W., and Davis, D. D.: Atmospheric chemistry results from the ANTCI 2005 Antarctic plateau airborne study, *J. Geophys. Res.-Atmos.*, 115, D07304,
25 doi:10.1029/2009JD012605, 2010.

Stull, R. B.: *An Introduction to Boundary Layer Meteorology*, Kluwer, Dordrecht, 1988.

Ullerstam, M., Thornberry, T., and Abbatt, J. P. D.: Uptake of gas-phase nitric acid to ice at low partial pressures: evidence for unsaturated surface coverage, *Faraday Discuss.*, 130,
30 211–226, doi:10.1039/B417418F, 2005.

Ulrich, T., Ammann, M., Leutwyler, S., and Bartels-Rausch, T.: The adsorption of peroxyntiric acid on ice between 230 K and 253 K, *Atmos. Chem. Phys.*, 12, 1833–1845, doi:10.5194/acp-12-1833-2012, 2012.

Weinheimer, A. J., Campos, T. L., Walega, J. G., Grahek, F. E., Ridley, B. A., Baumgardner, D., Twohy, C., and Gandrud, B.: Uptake of NO_y on wave-cloud ice particles, *Geophys. Res. Lett.*, 25, 1725–1728, 1998.

Ziereis, H., Minikin, A., Schlager, H., Gayet, J. F., Auriol, F., Stock, P., Baehr, J., Petzold, A., Schumann, U., Weinheimer, A., Ridley, B., and Strom, J.: Uptake of reactive nitrogen on cirrus cloud particles during INCA, *Geophys. Res. Lett.*, 31, L05115, doi:10.1029/2003GL018794, 2004.

ACPD

14, 12771–12796, 2014

HO_2NO_2 and HNO_3 in the coastal Antarctic winter night

A. E. Jones et al.

Title Page

Abstract

Introduction

Conclusions

References

Tables

Figures



Back

Close

Full Screen / Esc

Printer-friendly Version

Interactive Discussion



HO₂NO₂ and HNO₃ in the coastal Antarctic winter night

A. E. Jones et al.

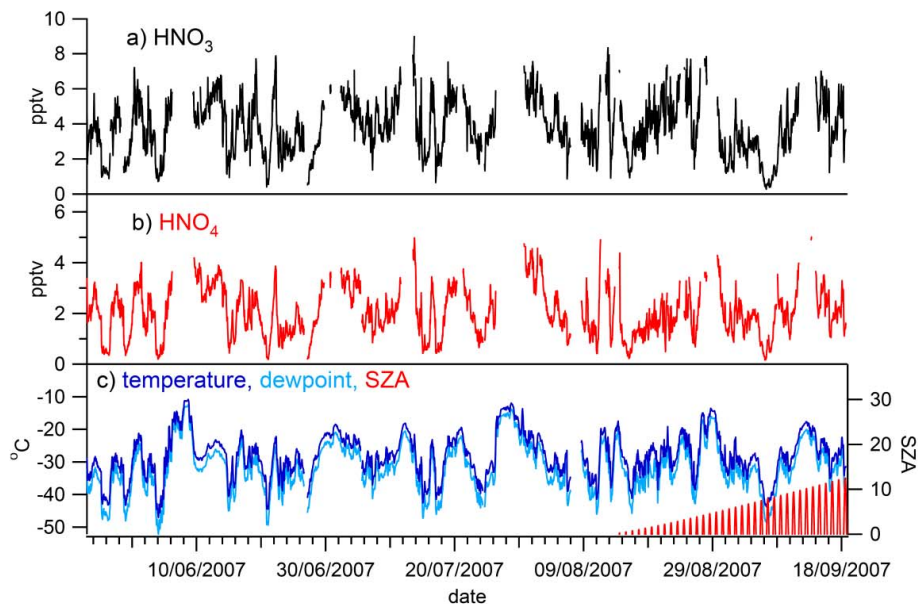


Figure 1. Time series of HNO₃, HO₂NO₂, ambient temperature, dewpoint, and solar zenith angle (SZAs) (hourly averages) for the entire measurement period discussed in this paper, 24 May 2007 to 18 September 2007.

[Title Page](#)[Abstract](#)[Introduction](#)[Conclusions](#)[References](#)[Tables](#)[Figures](#)[Back](#)[Close](#)[Full Screen / Esc](#)[Printer-friendly Version](#)[Interactive Discussion](#)

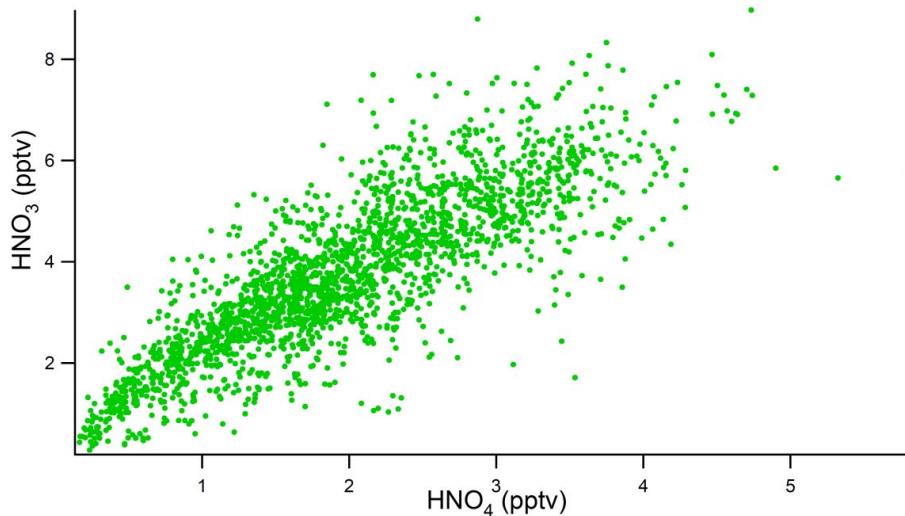


Figure 2. Nitric acid vs. peroxy nitric acid; 1-hourly averages of measurements made from 24 May 2007 to 18 September 2007.

HO₂NO₂ and HNO₃ in the coastal Antarctic winter night

A. E. Jones et al.

Title Page

Abstract

Introduction

Conclusions

References

Tables

Figures

◀

▶

◀

▶

Back

Close

Full Screen / Esc

Printer-friendly Version

Interactive Discussion



HO₂NO₂ and HNO₃ in the coastal Antarctic winter night

A. E. Jones et al.

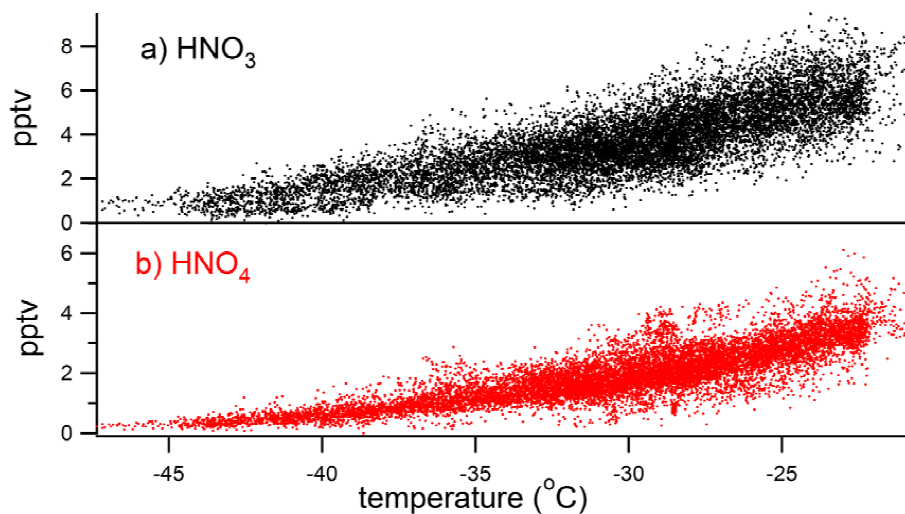


Figure 3. Nitric acid and peroxy nitric acid vs. ambient temperature; 10 min averages of measurements made from 24 May 2007 to 18 September 2007.

[Title Page](#)[Abstract](#)[Introduction](#)[Conclusions](#)[References](#)[Tables](#)[Figures](#)[Back](#)[Close](#)[Full Screen / Esc](#)[Printer-friendly Version](#)[Interactive Discussion](#)

HO₂NO₂ and HNO₃ in the coastal Antarctic winter night

A. E. Jones et al.

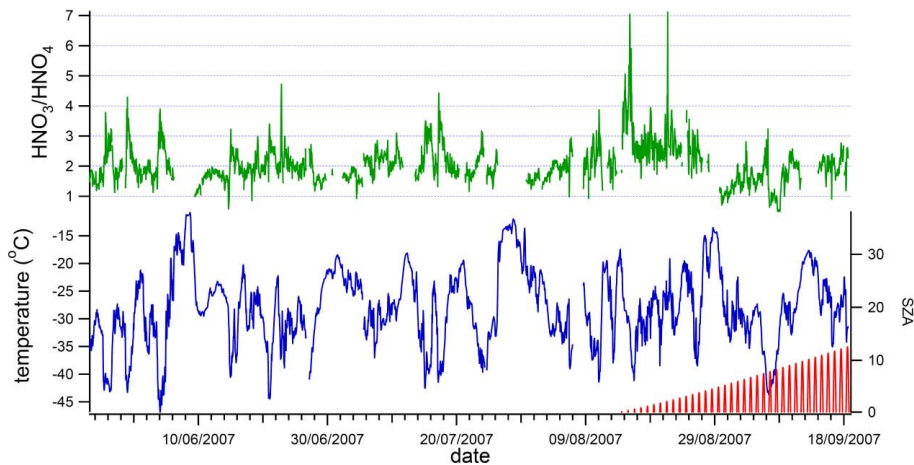


Figure 4. Ratio of HNO₃ : HO₂NO₂ (hourly average data) for the May to September measurement period. Also shown, for reference, are ambient temperature and solar zenith angle.

[Title Page](#)[Abstract](#)[Introduction](#)[Conclusions](#)[References](#)[Tables](#)[Figures](#)[Back](#)[Close](#)[Full Screen / Esc](#)[Printer-friendly Version](#)[Interactive Discussion](#)

HO₂NO₂ and HNO₃ in the coastal Antarctic winter night

A. E. Jones et al.

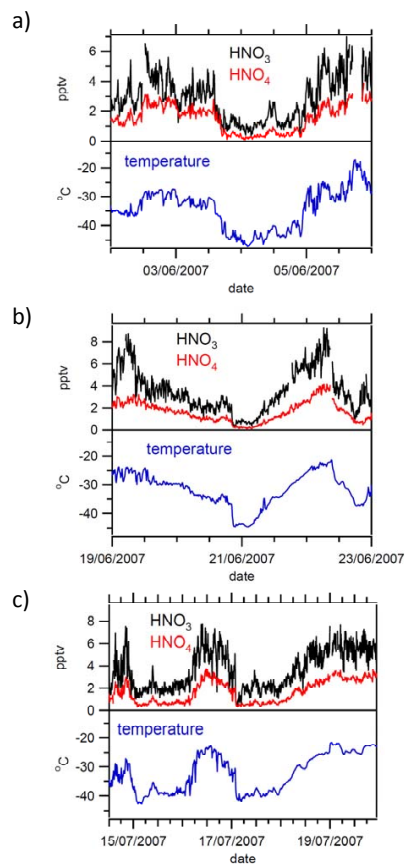


Figure 5. Three examples of short-term variability in HNO₃, HO₂NO₂ and ambient air temperature (10 min data), from (a) early June; (b) mid June; (c) mid July. All three periods are during the winter 24 h per day darkness.

HO₂NO₂ and HNO₃ in the coastal Antarctic winter night

A. E. Jones et al.

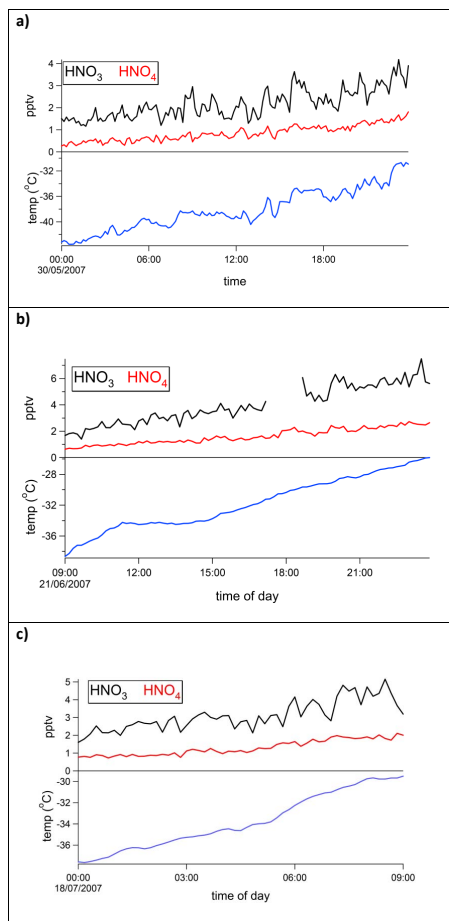


Figure 6. Detail of changes in HNO₃, HO₂NO₂ and temperature on **(a)** 30 May, **(b)** 21 June, and **(c)** 18 July. These three periods in the measurement series were characterised by low and invariant wind speeds and 24 h per day darkness.

HO₂NO₂ and HNO₃ in the coastal Antarctic winter night

A. E. Jones et al.

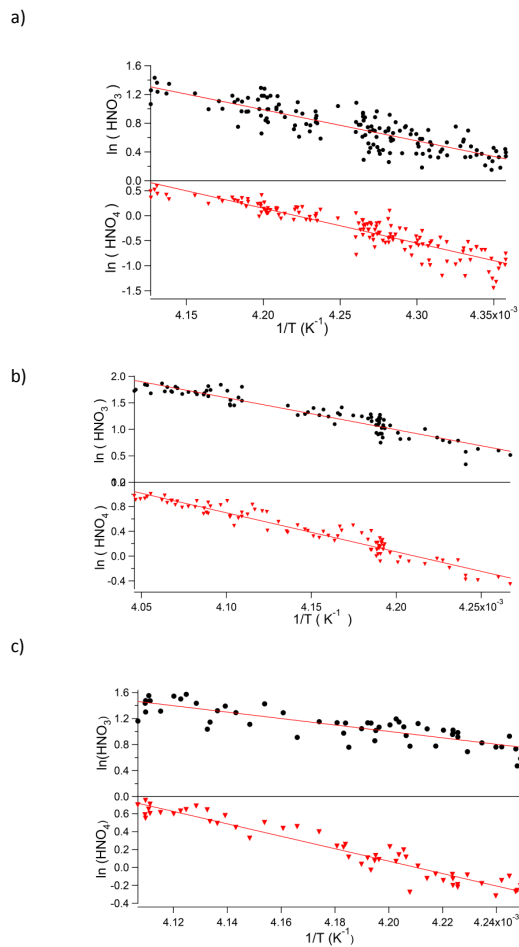


Figure 7. Plots of $\ln(\text{HNO}_3)$ and $\ln(\text{HO}_2\text{NO}_2)$ vs. $1/T$ for the time periods shown in Fig. 6, i.e. **(a)** 30 May, **(b)** 21 June, and **(c)** 18 July.

[Title Page](#)[Abstract](#)[Introduction](#)[Conclusions](#)[References](#)[Tables](#)[Figures](#)[Back](#)[Close](#)[Full Screen / Esc](#)[Printer-friendly Version](#)[Interactive Discussion](#)